

全固态 289.9 nm 紫外激光器的研究

王金艳¹, 李世杰¹, 刘天红^{1,2}, 郑权^{1,2}, 陈曦^{1*}, 陈磊¹, 王东贺¹¹长春新产业光电技术有限公司, 吉林 长春 130103;²中国科学院长春光学精密机械与物理研究所, 吉林 长春 130033

摘要 报道了全固态脉冲运转腔外四倍频 289.9 nm 紫外激光器。首先, 基于 Nd:KGW 晶体的受激拉曼散射机制, 以 Nd:YVO₄ 晶体作为增益介质, 结合声光调 Q 技术, 研制了一台 1159.31 nm 红外拉曼激光器。当二极管阵列的总抽运功率为 20 W 时, 1159.31 nm 激光的输出功率为 983 mW, 脉宽为 13.5 ns。依次利用 I 类相位匹配偏硼酸锂 (LBO) 和偏硼酸钡 (BBO) 晶体进行腔外二倍频和四倍频, 实现了平均功率为 108 mW 的 289.9 nm 紫外激光输出, 重复频率为 10 kHz, 脉冲宽度为 8 ns, 峰值功率为 1.35 kW, 四倍频转化效率为 11%。测量了紫外激光的输出光斑, 分析了平均功率随脉冲频率的变化关系。

关键词 激光器; 二极管抽运激光器; 拉曼激光器; 紫外激光; 声光调 Q

中图分类号 TN248.1

文献标识码 A

doi: 10.3788/CJL202249.0701001

1 引言

紫外波段激光器具有波长短、单光子能量高、热效应低等优点, 在光谱分析、光存储、微细制造中具有独特优势, 受到了研究者的广泛关注^[1-2]。

早期实现 289 nm 激光的方法是采用 532 nm 激光泵浦染料获得基频光, 再利用 CLBO (CsLiB₆O₁₀) 晶体进行倍频。1997 年, Chandra 等^[3]利用此方法获得了重复频率为 10 Hz, 单脉冲能量为 44 mJ 的 284~294 nm 调谐激光。2002 年, Johnston 等^[4]利用偏硼酸钡 (BBO) 晶体对铜蒸气激光器输出的 510 nm 和 578 nm 激光进行倍频, 输出了 255 nm 及 289 nm 紫外激光, 经实验证实, 289 nm 激光是用于剥离光纤外层聚合物和写入光纤光栅的理想光源。但这两种方法都存在缺陷, 染料激光器安全性差、耗能高、冷却系统复杂; 铜蒸气激光器的电热装置温度高达 1500 °C, 需要使用耐高温且真空气密性良好的氧化铝材料作外壳, 激光器极高的工作温度给使用过程增加了危险性和难度。

拉曼散射是一种非线性光学效应, 物质分子与光子之间发生非弹性散射, 散射光子的频率向低频方向移动的过程为斯托克斯 (Stokes) 散射, 反之为

反斯托克斯 (反 Stokes) 散射。受激拉曼散射过程使散射具有受激发射的性质。当频率为 ν_0 的基频光入射到拉曼介质时, 由于受激拉曼散射, 激光器内产生了频率为 ν_{s1} 的一阶 Stokes 光子, 当一阶 Stokes 光强达到阈值时, 将一阶 Stokes 光作为激发光, 产生频率为 ν_{s2} 的二阶 Stokes 光。依次类推, 这种效应称为级联受激拉曼散射。通过激光与拉曼介质的相互作用, 可实现激光的频率转换, 得到一些特殊频率的新型激光^[5]。

拉曼介质是拉曼激光器的核心, 常见的固体拉曼介质主要是钒酸盐和钨酸盐类晶体, 如掺钕钒酸钇 (Nd:YVO₄)、掺钕钨酸钾钪晶体 (Nd:KGW)、掺钕钒酸钪晶体 (Nd:GdVO₄) 等^[6-9]。2011 年, Yang 等^[10]以 Nd:YAG 作为激光工作物质, 通过 Cr:YAG 被动调 Q 方式, 利用 Nd:KGW 晶体的腔内受激拉曼效应, 实现了 1178 nm 激光输出, 当抽运二极管功率为 5.74 W 时, 频率为 10 kHz, 平均功率为 336 mW。2017 年, Dashkevich 等^[11]利用 Nd:KGW 晶体的自拉曼效应, 采取侧面抽运结构, 获得了单脉冲能量为 11.5 mJ、脉冲宽度为纳秒及亚纳秒量级的 1351 nm 人眼安全激光。2019 年, Yang 等^[12]利用皮秒 1064 nm 基频光激发 Nd:KGW 晶体的拉曼效

收稿日期: 2021-07-12; 修回日期: 2021-08-16; 录用日期: 2021-09-01

通信作者: *chenxi@cnilaser.com

应,获得了 1.01 W 拉曼激光,转换效率为 23.1%。

本文利用激光二极管阵列抽运 Nd:YVO₄ 晶体,结合声光调 Q 技术,通过拉曼介质选择及谐振腔镜膜系设计,得到了 1159.31 nm 一阶拉曼激光。产生的 1159.31 nm 红外脉冲激光被聚焦透镜聚焦到两个不同匹配角度的偏硼酸锂(LBO)和偏硼酸钡晶体中,分别产生了二次谐波和四次谐波,最终获得了平均功率为 108 mW 的 289.9 nm 紫外脉冲激光输出。

2 实验设计与装置

Nd:KGW 晶体是各向异性双轴晶体。当入射光沿晶体 N_p 轴传播且电矢量 E 平行于 N_m 轴时,在 1064 nm 激光激发下,拉曼频移量 901 cm^{-1} 附近的增益系数为 3.5 cm/GW ,线宽为 5.4 cm^{-1} ;当电矢量 E 平行于 N_g 轴时,拉曼频移量为 768 cm^{-1} ,增益系数为 4.4 cm/GW ,线宽为 6.4 cm^{-1} 。对应的

表 1 四倍频晶体参数

Table 1 Crystal parameters for fourth harmonic generation

Nonlinear crystal	Transmission range /nm	I-type phase-matching angle		Walk off angle /mrad	$d_{\text{eff}}/(\text{pm}\cdot\text{V}^{-1})$
		$\theta /(^{\circ})$	$\varphi /(^{\circ})$		
LBO	150–2600	90	69.4	12.92	0.326
BBO	189–3300	42.4	0	83.54	1.85
CLBO	180–2750	53.3	0	37.17	0.7
KABO	180–3780	50.2	0	52.07	0.316
KBBF	147–3660	33.3	0	59.06	0.422
RBBF	151–3500	36.3	0	54.4	0.389

实验装置如图 1 所示,抽运源为光纤耦合输出的激光二极管(LD)阵列,中心波长为 808 nm,最大输出功率为 20 W。C1 为 Nd:YVO₄ 晶体,Nd³⁺ 离子的掺杂浓度(原子数分数)为 0.1%,长度为 10 mm,双面镀抗反(AR)膜@808 nm & 1064 nm。C2 为 Nd:KGW 晶体,Nd³⁺ 离子的掺杂浓度(原子数分数)为 5%,长度为 20 mm,双面镀 AR 膜@1064 nm & 1159 nm。M1 为平面镜,镀有 AR 膜@808 nm 和高反(HR)膜@1064 nm & 1159 nm。M2 为平面镜,镀有 HR 膜@1064 nm,在 1159 nm 处的透过率为 30%。对于小脉宽高功率的调 Q 激光器,较高的透过率有利于实现高效率的短脉冲激光输出,M1 及 M2 的透过率曲线如图 2 所示。谐振腔采用平行平面腔,目的是获得较小发散角的输出光束。Q 为声光 Q 开关。谐振腔几何长度为 90 mm。F 为凸透镜,镀有 1159 nm AR 膜。LBO 晶体的相位匹配角度为 $\theta=90^{\circ}$, $\varphi=5.1^{\circ}$ 。BBO 晶体的相位匹配角度为 $\theta=42.4^{\circ}$, $\varphi=0^{\circ}$ 。C1、C2、LBO、BBO

中心波长分别为 1176.8 nm 和 1158.7 nm。为了获得 289 nm 紫外光,本文选用 Nd:YVO₄ 晶体作为增益介质来产生 1064 nm 线偏振光,同时以沿 N_p 轴切割的 Nd:KGW 晶体作为拉曼介质,且保证基频光偏振方向平行于 N_g 轴。

对于二倍频非线性晶体,我们选择生长技术比较成熟的 LBO 晶体。首先,以 Nd:KGW 产生的拉曼光为线偏振光,选用 I 类相位匹配,提高转化效率。其次,经理论计算,LBO 晶体在 1159 nm 波长处的倍频走离角为 3.06 mrad,小的走离角产生的二次谐波光束质量好,有利于提高四倍频效率。常见的可用于紫外波段的非线性晶体及其用于四倍频时的参数如表 1 所示,其中 CLBO 为硼酸锂铯,KBBF 为氟硼铍酸钾,RBBF 为氟硼铍酸铷。可以看出,BBO 的有效非线性系数(d_{eff})大约是其其他晶体的 6 倍,综合考虑我们选择 BBO 作为四倍频晶体。

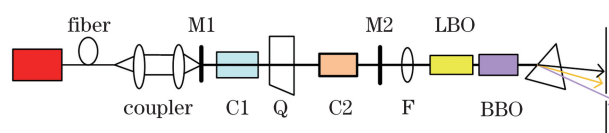


图 1 实验装置图

Fig. 1 Experimental setup

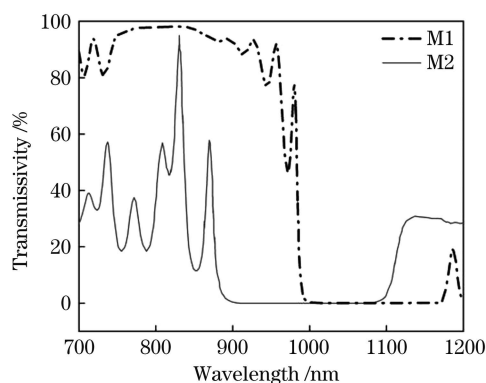


图 2 M1 和 M2 的透过率曲线

Fig. 2 Transmittance curves of M1 and M2

被放置于紫铜卡具中,由半导体制冷器(TEC)分别控制温度。最后利用三角棱镜使输出光沿不同的方向传播,便于测量紫外激光的各项参数。

激光器的运行过程如下。Nd:YVO₄晶体受到半导体抽运源的激发,通过声光Q开关对谐振腔内的损耗进行调制,在谐振腔内产生了1064 nm脉冲基频光振荡,由于Nd:KGW晶体的受激拉曼散射效应,激光器内产生了一阶斯托克斯光。一阶斯托克斯光通过M1、M2组成的谐振腔后反馈增强,最终由M2输出脉冲拉曼激光。经聚焦镜F聚焦后,倍频晶体LBO和四倍频晶体BBO顺次放在透镜焦点附近,分别实现了579 nm黄光输出和289 nm紫外激光输出。实验过程中精细调节LBO晶体和BBO晶体在透镜焦点附近的位置和角度,使紫外激光的输出功率最大。

3 实验结果

采用RGB Photonics公司生产的Qred系列光谱仪,测量范围为900~1700 nm。测试拉曼激光输出波长为1159.31 nm,如图3所示。增加抽运功率,拉曼激光的平均功率随之线性增长,变化关系曲线如图4所示。当总抽运功率为20 W时,平均输出功率

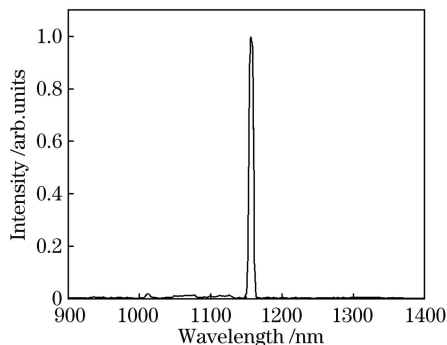


图3 拉曼激光光谱图

Fig. 3 Raman laser spectrum

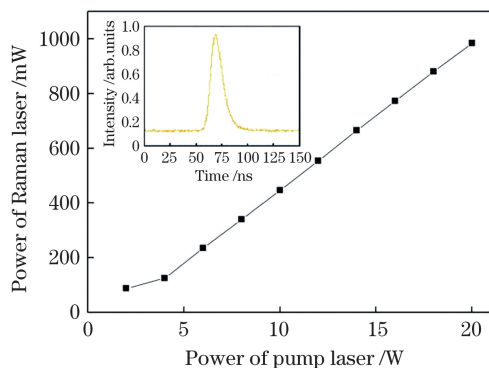


图4 输出功率随抽运功率的变化及脉冲波形

Fig. 4 Output power versus pump laser power and pulse waveform

为983 mW,调Q频率为10 kHz,脉宽为13.5 ns。

拉曼光经过BBO晶体和LBO晶体后,得到579.7 nm黄光和289.9 nm紫外激光,紫外激光光谱测量结果如图5所示。为了获得较高的四倍频转换效率,用焦距分别为40,60,100 mm的三种聚焦镜进行实验,与之对应获得了最高平均功率为55,108,88 mW的紫外激光。由此可见,并不是焦距越短效率越高。当焦距较短时,虽然拉曼光的功率密度大,但是焦深短,经LBO倍频后进入BBO晶体的二倍频光发散角更大,不利于四倍频的产生。若焦距过长,拉曼光和倍频光的功率密度都会降低,四倍频的效率也会降低。所以,选择透镜焦距需兼顾这两方面要素。

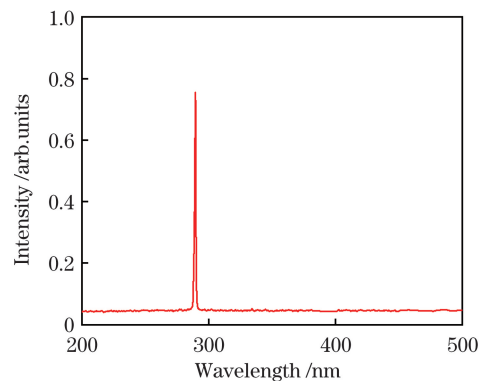


图5 紫外激光光谱

Fig. 5 Spectrum of ultraviolet laser

紫外激光输出光斑近似椭圆形,焦距为100 mm的聚焦镜对应的紫外激光光斑发散角更小,但四倍频转换效率为8.9%。焦距为60 mm时,转换效率为11%。图6给出了焦距为60 mm时二倍频与四倍频激光的输出功率随拉曼光功率的变化曲线,二者均随着抽运功率的增加呈递增趋势。调Q频率为10 kHz时,紫外激光的最高平均功率为108 mW,脉冲宽度为8 ns。测量了不同重复频率下的输出功率,结果如图7所示,重复频率小于

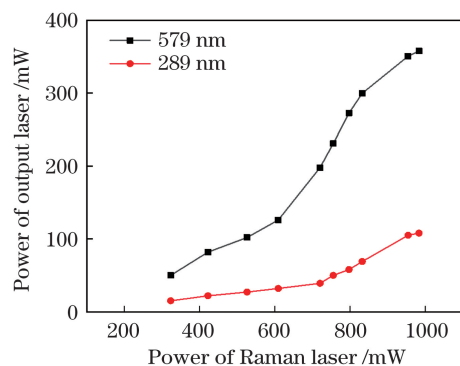


图6 二倍频光及紫外光输出功率曲线

Fig. 6 Output power curves of double frequency and ultraviolet lasers

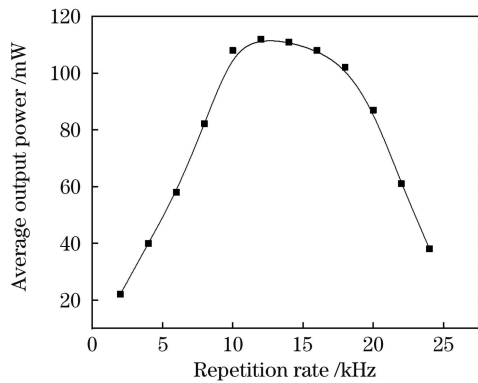


图 7 不同频率下的输出功率

Fig. 7 Output power at each frequency

10 kHz 时,紫外光的平均功率随频率的增大而增大,当频率为 10~16 kHz 时,平均功率变化不大,频率大于 16 kHz 时,功率逐渐下降。刀口法测量的出口处光斑尺寸为 0.48 mm×0.40 mm,水平方向发散角为 1.18 mrad,垂直方向发散角为 2.06 mrad。用狭缝扫描式光斑分析仪(Thorlabs BP209-VIS/M)测量光斑轮廓,考虑到测量仪器的损伤阈值,在距离激光出口 40 cm 处测量光斑分布,如图 8 所示。

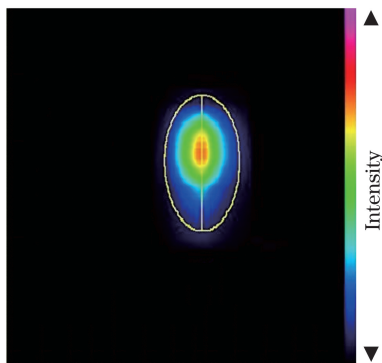


图 8 紫外激光光斑轮廓

Fig. 8 Ultraviolet laser spot profile

4 结 论

研制了一种全固态拉曼激光腔外四倍频 289.9 nm 紫外激光器。分析了 Nd:KGW 晶体的受激拉曼特性,采用腔内调 Q 受激拉曼方法获得了 1159.31 nm 一阶拉曼激光;采用 I 类相位匹配 LBO 晶体对以脉冲形式运转的拉曼激光进行倍频,实现了 579.7 nm 脉冲黄光激光输出,再利用 BBO 晶体四倍频方式,获得了 289.9 nm 紫外脉冲激光输出。比较了不同焦距的透镜对输出功率和光斑的影响。为了获得不同特性的紫外光,需选择不同的透镜参数。此方式获得的紫外光光斑小,且成本低,

系统运行稳定,是目前获得 289.9 nm 激光的最佳方式,为市场应用提供了便利条件。

参 考 文 献

- [1] Rios N P S M, de Azevedo L A, Neves R C S, et al. Synthesis of luminescent gel-like materials based on glutamate and neodymium (III) [J]. *Materials Letters*, 2018, 230: 69-71.
- [2] Fu X H, Chen C, Hu Z G, et al. Development of separation film for frequency doubling in 278 nm all-solid-state laser system [J]. *Chinese Journal of Lasers*, 2019, 46(12): 1203002.
付秀华, 陈成, 胡章贵, 等. 278 nm 全固态激光系统倍频分离膜的研制[J]. *中国激光*, 2019, 46(12): 1203002.
- [3] Chandra S, Allik T H, Hutchinson J A, et al. Tunable ultraviolet laser source based on solid-state dye laser technology and CsLiB₆O₁₀ harmonic generation[J]. *Optics Letters*, 1997, 22(4): 209-211.
- [4] Johnston B F, Lee A J, Withford M J, et al. Laser assisted jacket removal and writing of fiber Bragg gratings using a single laser source [J]. *Optics Express*, 2002, 10(16): 818-823.
- [5] Zhao H, Wang H Y, Zhu S Q, et al. 578.5 nm end-pumped passively Q-switched Raman yellow laser [J]. *Laser & Optoelectronics Progress*, 2021, 58(1): 0114004.
赵辉, 王浩宇, 朱思祁, 等. 578.5 nm 端面泵浦被动调 Q 拉曼黄光激光器[J]. *激光与光电子学进展*, 2021, 58(1): 0114004.
- [6] Dashkevich V I, Shpak P V, Voitkov S V, et al. Eye-safe actively Q-switched diode-pumped lasers with intracavity Raman conversion in YVO₄, KGd(WO₄)₂, PbWO₄, and Ba(NO₃)₂ crystals [J]. *Optics Communications*, 2015, 351: 1-8.
- [7] Lin J P, Pask H M. Cascaded self-Raman lasers based on 382 cm⁻¹ shift in Nd:GdVO₄ [J]. *Optics Express*, 2012, 20(14): 15180-15185.
- [8] Frank M, Smetanin S N, Jelinek M, et al. Highly efficient picosecond all-solid-state Raman laser at 1179 nm and 1227 nm on single and combined Raman lines in a BaWO₄ crystal [J]. *Optics Letters*, 2018, 43(11): 2527-2530.
- [9] Kinyaevskiy I O, Kovalev V I, Danilov P A, et al. Highly efficient stimulated Raman scattering of sub-picosecond laser pulses in BaWO₄ for 10.6 μm difference frequency generation [J]. *Optics Letters*, 2020, 45(8): 2160-2163.
- [10] Yang H W, Zhao J X, Huang H T, et al. The first-

stokes pulse generation in Nd: KGW intracavity driven by a diode-pumped passively Q-switched Nd:YAG/Cr⁴⁺ laser [J]. *Laser Physics*, 2011, 21 (2): 343-347.

- [11] Dashkevich V I, Orlovich V A. Eye-safe KGd(WO₄)₂: Nd laser: nano- and subnanosecond pulse generation in self-frequency Raman conversion

mode with active Q-switching [J]. *Journal of Applied Spectroscopy*, 2017, 84(1): 40-45.

- [12] Yang C, Peng H P, Chen M, et al. 1 kHz dual sub-pulse train picosecond radially polarized beam KGW Raman generator capable of achieving multiple optical communication wavelength [J]. *Optics Communications*, 2019, 452: 481-486.

Research on All Solid-State Ultraviolet Laser at 289.9 nm

Wang Jinyan¹, Li Shijie¹, Liu Tianhong^{1,2}, Zheng Quan^{1,2}, Chen Xi^{1*}, Chen Lei¹, Wang Donghe¹

¹ Changchun New Industries Optoelectronics Technology Co., Ltd., Changchun, Jilin 130103, China;

² Changchun Institute of Optics, Fine Mechanics and Physics, Chinese Academy of Sciences, Changchun, Jilin 130033, China

Abstract

Objective Because of its advantages such as short wavelength, high single-photon energy and low thermal effect, an ultraviolet laser can be used in spectral analysis, optical storage, and micro-fabrication. The 289 nm laser has been proven to be an ideal light source for stripping the outer polymer of a fiber and writing a fiber grating. They can also be used for spectrophotometric separation and determination. In this paper, we have investigated a 289.9 nm ultraviolet laser based on frequency quadrupling of an Nd: KGW Raman laser with an external-cavity configuration. It is a new way to get 289.9 nm laser for a solid state laser. This laser has advantages of ultra-compact, easy operation, and low cost. By further optimizing the experiment, researchers can get better results.

Methods Nd:KGW is an efficient Raman crystal and has relatively low pumping threshold and a high Raman gain coefficient. If the exciting wave propagates along the N_p axis, it involves the strong Raman line at 786 cm^{-1} while the polarization is parallel to the N_g axis of the Nd: KGW crystal. LBO crystal is used for second harmonic generation (SHG). First, the Raman laser generated by Nd: KGW is linearly polarized and I-type phase matching can improve the conversion efficiency. Second, the theoretical walk-off angle of LBO is 3.06 mrad. A small walk-off angle produces a good beam quality, which is beneficial for fourth harmonic generation (FHG). For FHG, we compare the common ultraviolet nonlinear crystals and their parameters (Table 1). Taking everything into consideration, the BBO is chosen for FHG.

The experimental setup is designed (Fig. 1). The laser is end-pumped by a fiber-coupled diode array (LD) emitting at 808 nm. The diode emission is focused into the laser crystal by a pair of lenses (coupler). C1 is a Nd:YVO₄ crystal coated with anti-reflection (AR) @808 nm & 1064 nm coatings on both facets. C2 is a 20 mm long b-cut Nd:KGW Raman crystal. M1 is an input mirror. M2 is an output coupler coated with high reflection (HR) @1064 nm coating, and the transmittance at 1159 nm is 30%. The transmittance spectra for M1 and M2 from 700 nm to 1200 nm are designed (Fig. 2). Q is an acousto-optic Q switch. The geometric length of the cavity is 90 mm. The LBO crystal is deposited at the focus of the convex lens (F).

Results and Discussions The output wavelength of the Raman laser is 1159.31 nm (Fig. 3). The maximum average output power of 983 mW is obtained at a total pump power of 20 W with repetition rate of 10 kHz and pulse duration of 13.5 ns (Fig. 4). The pulse trains and temporal profiles under the maximum output power are displayed (Fig. 4). The maximum power of the yellow laser is up to 358 mW with pulse duration of 9.5 ns. The output wavelengths of the yellow and ultraviolet (UV) lasers are measured to be 579.7 nm and 289.9 nm (Fig. 5).

Three kinds of convex lenses with focal lengths of 40 mm, 60 mm, and 100 mm are used in the experiment, respectively. Correspondingly, the UV lasers with the highest average powers of 55 mW, 108 mW, and 88 mW are achieved. It can be seen that the shorter the focal length, the higher the efficiency. Although the power density of the Raman light is large with a shorter focal length, it also causes great divergence into the BBO crystal.

Alternately, if the focal length is too large, the power density of the Raman laser will be reduced, and the efficiency of FHG will also be reduced. Therefore, choosing the focal length of the lens should take into account these two factors.

The focal length of 100 mm corresponds to a small divergence angle, but the quadruple frequency conversion efficiency is 8.9%. When the focal length is 60 mm, the conversion efficiency is 11%. The relationships between the output powers of SHG and FHG lasers and the power of the Raman laser with a 60 mm focal length are measured (Fig. 6). The highest average power of the UV laser is 108 mW, and the pulse duration is 8 ns at 10 kHz. The output powers at different frequencies are shown (Fig. 7). When the repetition rate is less than 10 kHz, the average power increases with the frequency. The power changes a little between 10 kHz and 16 kHz. When the rate is greater than 16 kHz, it decreases gradually. Taking into account the damage threshold of the instrument, a scanning slit optical beam profiler is used to measure the spot distribution of the 289.9 nm laser 40 cm away from the exit (Fig. 8). The size of the spot at the exit measured by the knife-edge method is $0.48 \text{ mm} \times 0.4 \text{ mm}$. The horizontal divergence angle is 1.18 mrad, and the vertical divergence angle is 2.06 mrad.

Conclusions In summary, a pulsed ultra-violet laser at 289.9 nm with good beam-quality has been investigated. And based on the nonlinear conversion of type-I phase-matched LBO and BBO crystals for extra-cavity SHG and FHG, a 289.9 nm UV laser is achieved. The average output power is 108 mW with a repetition rate of 10 kHz and a pulse duration of 8.0 ns at a total pump power of 20 W.

Key words lasers; diode-pumped laser; Raman laser; ultraviolet laser; acousto-optic Q-switch